Effect of surface states of steel on microstructure and mechanical properties of lap joints of magnesium alloy and steel by friction stir welding

Y. C. Chen* and K. Nakata

AZ31 Mg alloy (top sheet) and steel (zinc coated steel and brushed finish steel) were friction stir lap welded, and the effect of surface states of steel on the microstructure and mechanical properties of joints was examined. The failure loads of the zinc coated steel joints could reach 2·3 kN. Mg alloy and brushed finish steel could not be welded in current experimental conditions. The presence of zinc coat promoted the formation of liquid low melting Mg–Zn eutectic products at the interface. The liquid products, as well as broken oxide films and surface contaminants, were forced out of the joining interface by the high pressure produced by the tool. As a result, fresh interfaces were exposed, which led to the mutual diffusion between magnesium alloy and steel. Findings of the present study suggest that the presence of zinc coat significantly improves the weldability in friction stir lap welding of magnesium alloy and steel.

Keywords: Friction stir welding, Magnesium alloy, Steel

Introduction

Magnesium alloys are increasingly being used in automobile structures, from seat frames and door frames to the auto body.[1,2] Steels are the first choice for structural components in the auto body.[1] The need of light weight in automotive body leads to the increasing use of the joining of magnesium alloy and steel in vehicle manufacture. Therefore, the development of reliable joints between magnesium alloy and steel becomes urgent, and the joining difficulties between magnesium alloy and steels must be faced.[1–4] It is difficult to join Mg alloys to steels by conventional fusion welding processes. Liu and Zhao[4] studied the lap joining of the dissimilar alloys of AZ31B Mg alloy and 304 steel by a laser Gas Tungsten Arc (GTA) hybrid welding technique. A transition zone formed at the interface of the Mg–Fe. The presence of transition zone deteriorated the mechanical properties of the joints. Therefore, the joints did not show high strength and fractured at the interface.

The friction stir welding (FSW) process[5] can weld Mg alloys[6–10] and steel[11–18] and achieve high quality joints than fusion welding technology. Good welds can be produced when FSW is used to join dissimilar materials of magnesium alloys and steels. Watanabe *et al.*[19] studied the weldability of FSW AZ31 magnesium alloy/SS400 steel and reported that the rotation speed, the position of the pin axis had a significant effect on the strength and the microstructure of the joint. Current studies only reported the weldability of solid state welding or fusion welding of magnesium alloy/steel and the preliminary results of mechanical properties and microstructure evolution of the joints.[4,19] Systematic research about the effect of the surface state of steel on the weldability of Mg alloy and steel has not been reported.

In the present study, 1·6 mm thick AZ31 magnesium alloy and two kinds of 0·8 mm thick steel sheets (zinc coated steel and brushed finish steel) are selected as the experimental materials for friction stir lap welding. The magnesium alloy sheet is put on the steel sheet. To eliminate the effect of the stir behaviour of the tool and highlight the effect of the surface states of steel on the weldability, a 1·5 mm long probe is selected so that the probe tip of the tool does not touch the surface of the steel sheet during welding. The tensile properties of joints and microstructural features in the lap interface are examined, and the effect of the surface state of steel on the weldability of Mg alloy and steel is discussed.

Experimental procedure

The base materials (BMs) used in this study were a 1·6 mm thick AZ31 magnesium alloy sheet and a 0·8 mm thick low carbon steel sheet. For comparison, two kinds of steel sheets were selected, i.e. zinc coated steel and brushed finish steel. The chemical composition and mechanical properties of the BMs are shown in

Joining and Welding Research Institute, Osaka University, 11-1 Mihogaoka, Ibaraki, Osaka 567-0047, Japan

*Corresponding author, email armstrong@hit.edu.cn

Published by Maney on behalf of the Institute
Received 25 August 2009; accepted 25 October 2009
DOI 10.1179/136217109X12568132624325

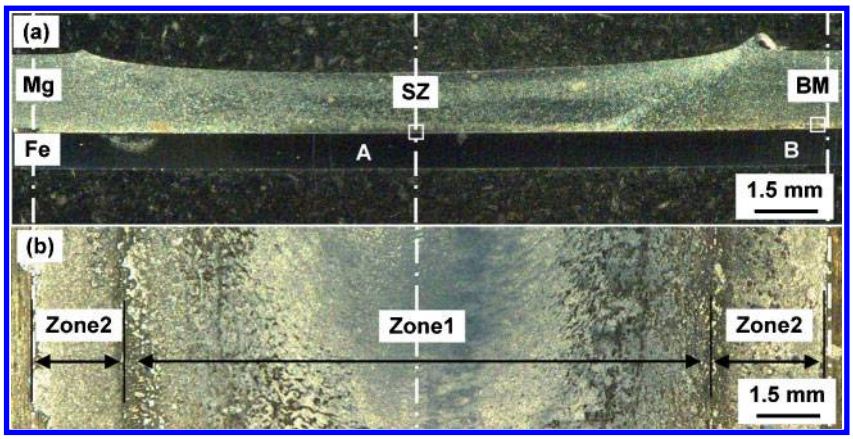

1 ***a*** **cross-sections of zinc coated steel joint and** ***b*** **front view of fracture surface at Mg alloy side; image shown are from fractured weld samples taken from top surface of bottom Mg sheet**

Table 1. Rectangular welding samples, 300 mm long by 100 mm wide, were lap welded using a FSW machine. The welding parameters were rotation speed of 25 rad s^{-1} and welding speeds of 3·3 and 5 mm s^{-1}. The upsetting force of the welding tool (made of SKD61 steel) was 3·92 kN. The shoulder diameter and probe diameter of the tool were 15 and 5 mm respectively. The length of the probe was 1·5 mm, and the welding tilt angle was 3°.

After welding, the joint was cross-sectioned perpendicular to the welding direction for the metallographic analysis and tensile tests using an electrical discharge cutting machine. The cross-sections of the metallographic specimens were mechanically ground with water abrasive paper and polished with 3 and 1 μm diamond, and observed by optical microscopy. The mechanical properties of the joint were measured using tensile tests. The tensile tests were carried out at room temperature at a crosshead speed of 0·0167 mm s^{-1} using a tensile testing machine, and the mechanical properties of the joint were evaluated using three tensile specimens cutting from the same joint. The shape of the test specimen was rectangular, and the width of each specimen was 20 mm.

The welding thermal cycle histories along the interface during FSW were measured by an array of K type thermocouples (0·2 mm diameter) at various locations from the weld centre. Microstructure characteristic and element distribution along the interface were analysed by SEM equipped with an energy dispersive X-ray spectroscopy (EDS) analysis system. Fracture surfaces of joints were analysed using X-ray diffraction (XRD) after tensile test.

Experimental results

Table 2 shows the tensile shear strengths and fracture locations of lap joints of AZ31 magnesium alloy with two kinds of steels. Tensile test results show that surface states of steel have a significant effect on the mechanical properties of lap joints welded with the same welding parameters. Joints of zinc coated steel fracture at the interface, with failure loads reaching 2·3 kN. Joints of brushed finish steel split during preparation of tensile test samples. It indicates that the presence of zinc coat greatly improves the friction stir lap weldability of magnesium alloy and steel.

The macroscopic view of traverse section of zinc coated steel joints is shown in Fig. 1*a*. Figure 1*b* presents the front view of the fracture surface of the magnesium alloy. It can be seen from Fig. 1*a* that magnesium alloy and steel are tightly joined. Microstructure at the side of magnesium alloy is characteristic of friction stir welded magnesium alloy. In this study, we are mainly concerned about structure at the interface. From the typical fracture surface of the joint (seen in Fig. 1*b*), it can be seen that two significant zones are produced after welding. For convenience's sake, the two zones are defined as zone 1 and zone 2. Obviously, the width of zone 1 exceeds the length of the probe diameter. Zone 2 presents characteristics of resolidifying process. The total width of bonding land (zone 1 + zone 2) is about 19 mm, wider than that of the shoulder diameter.

The macroscopic view of traverse section of brush finished steel joints is shown in Fig. 2*a*. Figure 2*b* presents the front view of the fracture surface of the magnesium alloy. The microstructure at the interface is quite different from that of zinc coated steel joints. From the fracture surface of the joint, we can see that only one zone is produced after welding. The width of this zone is ~3·5 mm, slightly smaller than the length of the probe diameter. It indicates that surface states of steel have a significant effect on the width of bonding land of magnesium alloy/steel lap joints.

Figure 3 shows the microstructure at the centre of lap interface (position A shown in Fig. 1*a*) of magnesium alloy and zinc coated steel. It can be seen from Fig. 3*a*

Table 1 Chemical compositions and mechanical properties of base materials (BMs)

	Chemical composition, mass%										Mechanical properties	
BMs	Al	Cu	Mn	Fe	C	Mg	Ni	P	Zn	S	Strength, MPa	Elongation, %
AZ31	3	…	0·2	…	…	Bal.	…	…	1	…	239	13
Zn coated steel	0·06	0·02	0·20	Bal.	0·04	…	0·01	0·013	…	0·005	328	33·4

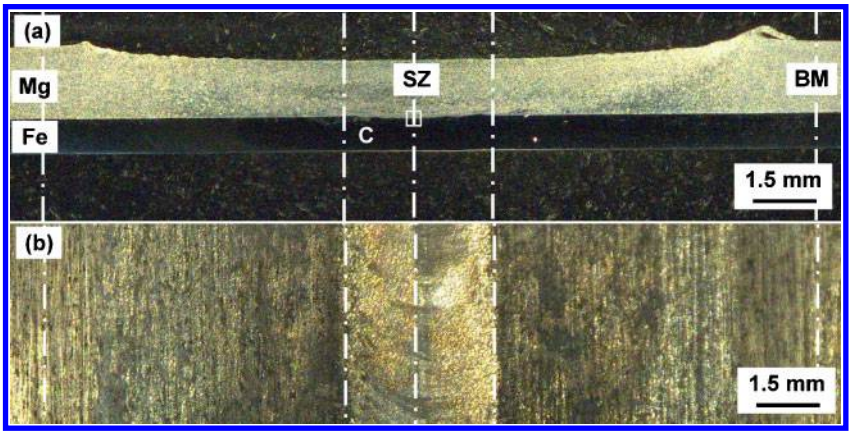

2 ***a*** **cross-sections of brushed finish steel joint and** ***b*** **front view of fracture surface at Mg alloy side; image shown are from fractured weld samples taken from top surface of bottom Mg sheet**

that structure of the joint consists of three layers, i.e. microstructure in stir zone of magnesium alloy, an intermetallic compound (IMC) layer and BM of steel. The representative concentration profiles of Mg, Zn, Al and Fe cross the interface between magnesium alloy and steel are shown in Fig. 3*b*–*e*. Zn has not been detected, while plenty of Al has been found. The result suggests that it is possibly at the bonding interface that IMC of Al/Mg or Al/Fe forms.

Figure 4 shows the microstructure at position B shown in Fig. 1*a*. There is solidified structure in the gap between magnesium alloy and zinc coated steel. As shown in Fig. 1*a*, this position has slightly exceeded the domain of shoulder diameter of the tool. The representative concentration profiles of Mg, Zn, O and Fe cross the interface are shown in Fig. 4*b*–*e*. The concentration profiles of Mg and Zn detected in this region indicates the possible presence of Mg–Zn eutectic structure (ES). There are two kinds of phases in this zone, the white substrate and the black massive phase. Quantitative analysis of the chemical compositions by EDS shows that the black massive phase consists of 80·1 at.-%Mg, 11 at.-%O and 8·9 at.-%Zn, while the white substrate contains 62·56 at.-%Mg, 5·7 at.-%O and 31·73 at.-%Zn. This result suggests that the black phase is primary phase Mg, and the white substrate is Mg_7Zn_3. Meanwhile, this zone shows an apparent O rich characteristic. It suggests that liquid ES with O rich products flows to this position during FSW.

Figure 5 shows microstructure at the centre of lap interface of magnesium alloy and brushed finish steel. The typical concentration profiles of Mg, Al and Fe cross the interface are shown in Fig. 5*b*–*d*. It can be seen that there is no IMC layer at the interface. Magnesium metal is pushed into the concavities of the brushed finish steel surface. Magnesium alloy and steel are joined through some kind of mechanical bonding, and the bonding land is only under the domain of the probe diameter (see Fig. 2*b*).

To detect whether IMC forms at the interface, X-ray diffraction patterns from fractured surfaces of the magnesium alloy and steel are analysed. X-ray diffraction analysis results are shown in Fig. 6. For zinc coated steel joints, diffraction lines from IMC of Fe4Al13 are detected at the steel side. At the same time, elements of Mg and Fe from BMs are also detected. For brushed finish steel joints, only elements of Mg and Fe are detected. This result indicates that no IMC form at the interface, when the brushed finish steel is selected as BM in current experimental conditions. The joining between magnesium alloy and brushed finish steel is made through mechanical bonding.

Table 2 Tensile test results of steel BMs and FSW joints

Joint type	Failure load	Fracture location
Zinc coated steel joints (3·33 mm s^{-1})	2·3 kN	Interface
Zinc coated steel joints (5 mm s^{-1})	0·6 kN	Interface
Brushed finish steel joints (3·33 mm s^{-1})	…	Interface
Brushed finish steel joints (5 mm s^{-1})	…	Interface

Discussion

Microstructure analysis and mechanical properties test results show that surface states of steel have a significant effect on the friction stir lap weldability of magnesium alloy and steel. For solid state bonded joint of dissimilar metals, there are two main factors controlling the joining performance.[20] One is the intimate contact between dissimilar materials, and the other is the microstructure, particularly the formation of IMCs. In the present experiment, the surface of steel does not get any surface treatment before welding so that the effect of the original surface state of steel on the weldability could be studied. No fresh metal surface is exposed before welding, so there is no intimate contact between magnesium alloy and steel. For brushed finish steel joints, there are lots of concavities on the rough surface of steel. The magnesium alloy is pushed into these concavities during FSW. Magnesium alloy and steel are joined through mechanical bonding, and the bonding land is only under the domain of the probe diameter. Therefore, brushed finish steel joints do not exhibit considerable failure load. However, for zinc coated steel joints, the joints exhibit considerable failure load compared with the brush finished steel joints. Obviously, the presence of zinc coat significantly improves the weldability of magnesium alloy and steel. As we know, the metal in the lap interface undergoes the synthetic effect of the thermal cycle and the mechanical cycle during FSW because of the action of friction, stir and extrusion of the tool. Thus, high temperature and high pressure are generated at the interface. Welding

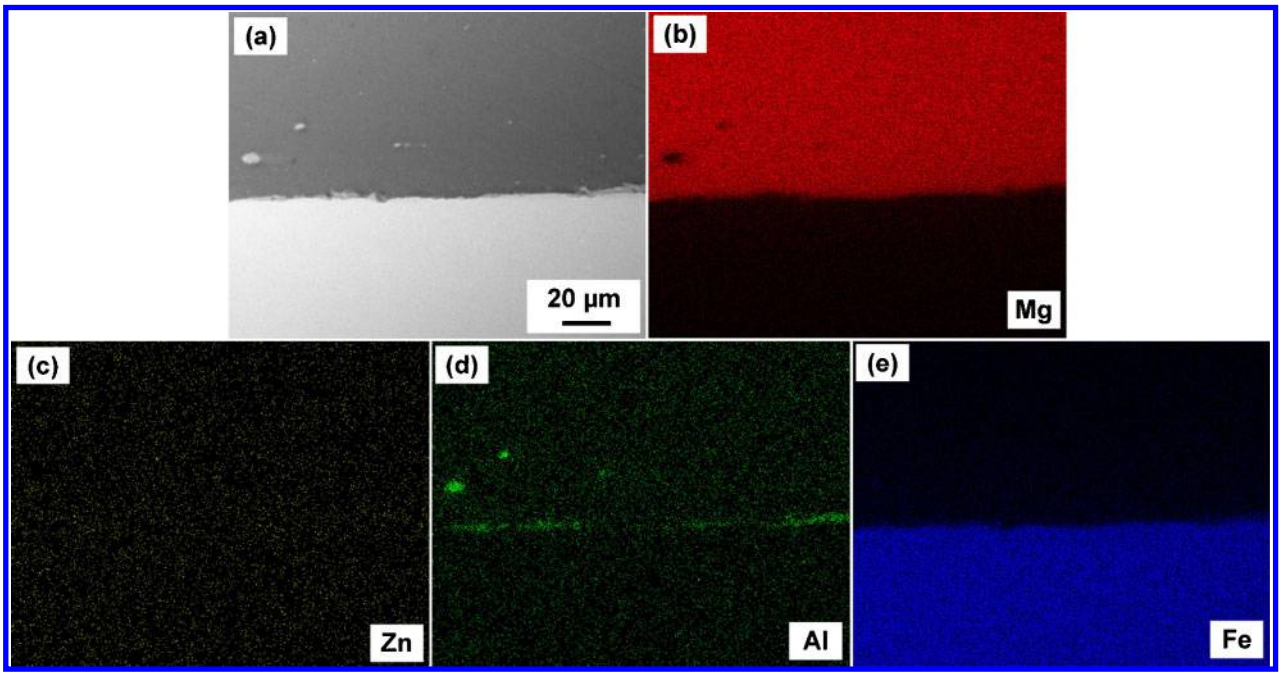

3 SEM and EDS analysis results at position A shown in Fig. 1*a*

heat cycle histories are measured with an array of K type thermocouples during FSW. The measure positions are shown in Fig. 7. The peak temperatures at positions of 0, 8 and 20 mm are about 522, 450 and 136°C respectively. Such temperatures are lower than the melting points of Mg and Fe BMs (648 and 1538°C respectively),[21] but higher than the melting point of Zn and Mg–Zn eutectic point (420 and 339°C respectively).[21] In other words, the peak temperature in the lap interface centre is higher than the melting point of Zn and Mg–Zn eutectic point, which results in the formation of a liquid phase. The joining mechanism of magnesium alloy and zinc coated steel are explained below. High temperature first leads to the melting of zinc coat, and high pressure simultaneously results in the rupture of surface oxide films at both sheets' surface, which promotes the formation of low melting Mg–Zn eutectic products. High pressure then forces the liquid Mg–Zn eutectic reaction products, as well as broken oxide films and surface contaminants, to move far away from the weld centre. These mixture spread along the interface and then pile into the natural gap between two sheets. In this way, the fresh interfaces are exposed, and they are tightly extruded together after the liquid phase is pushed out. There is mutual diffusion of Mg/Fe and Al/Fe, which leads to the formation of a new IMC at the lap interface.

Conclusion

AZ31 magnesium alloy and two kinds of steels were lap welded using FSW technology. The effect of surface

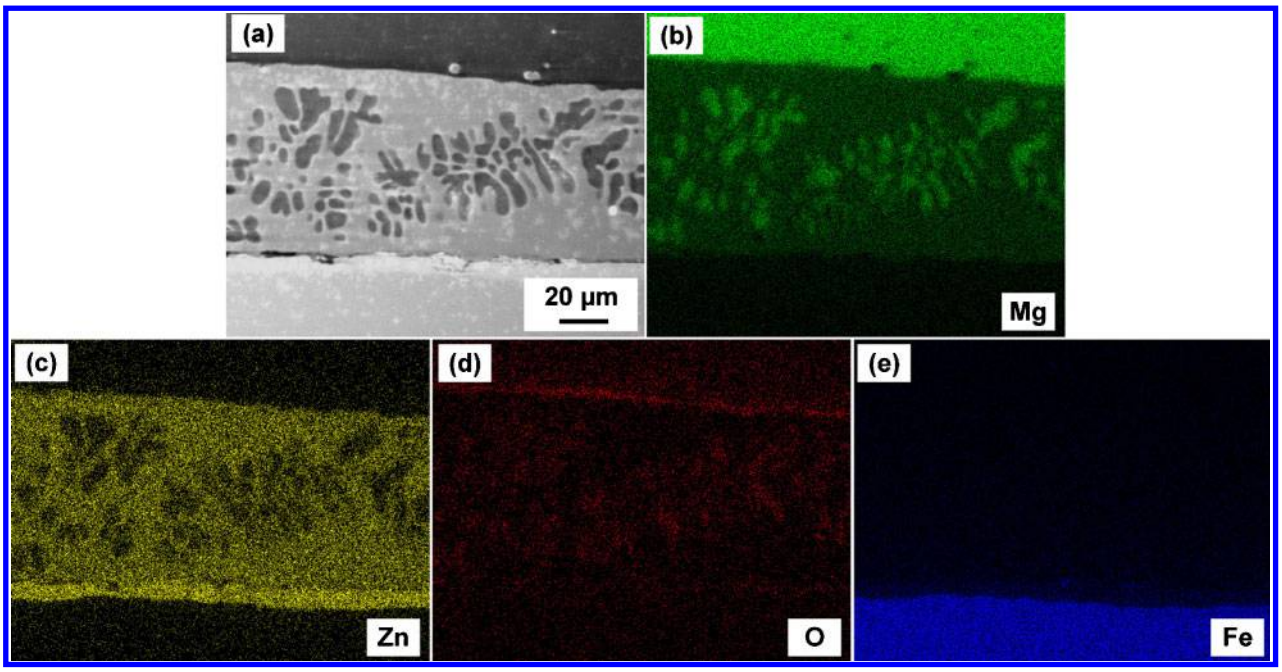

4 SEM and EDS analysis results at position B shown in Fig. 1*a*

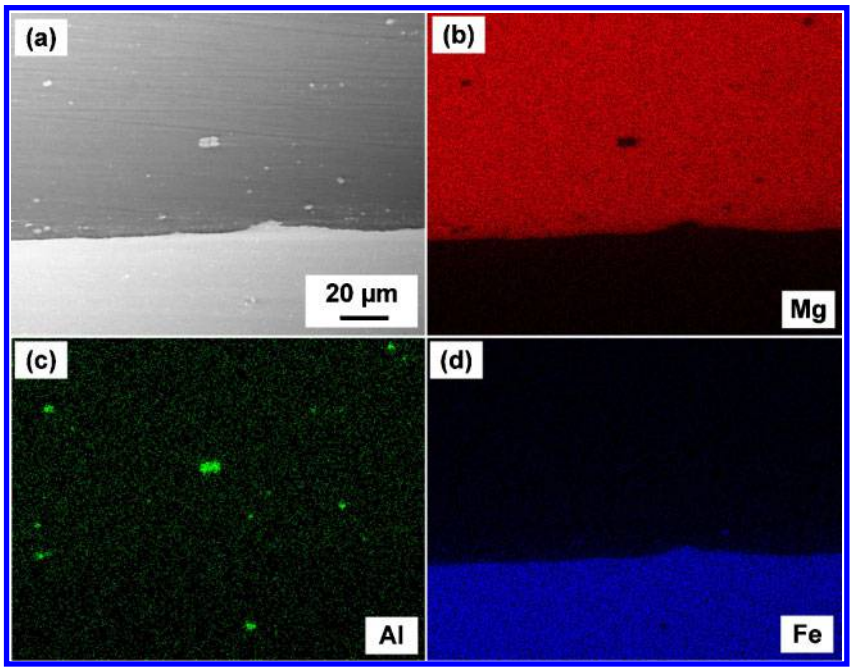

5 SEM and EDS analysis results at position C shown in Fig. 2*a*

states of steels on the weldability of magnesium alloy and steel was investigated.

The AZ31/zinc coated steel joints showed higher failure loads than the AZ31/brushed finish steel joints, which proves that the presence of zinc coat significantly improved the weldability of magnesium alloy and steel. The appearance and extrusion of low melting eutectic phase at the interface led to the exposure of fresh metal surface, which increased the mutual diffusion between magnesium alloy and steel.

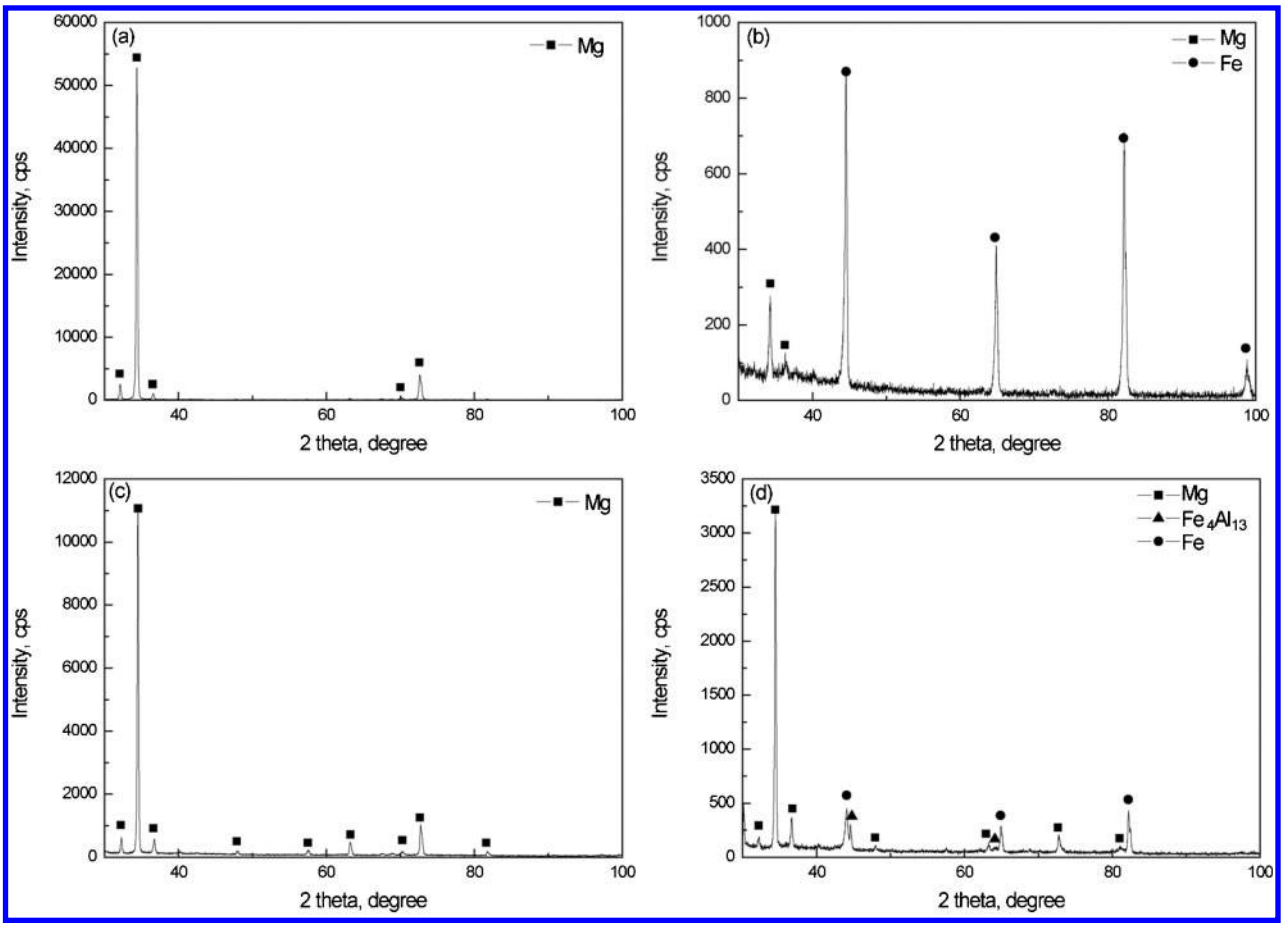

6 X-ray diffraction analysis results from fracture surface of joints (3·33 mm s^{-1}) *a* from Mg side of brushed finish steel joint; *b* from Fe side of brushed finish steel joint; *c* from Mg side of zinc coated steel joint and *d* from Fe side of zinc coated steel joint

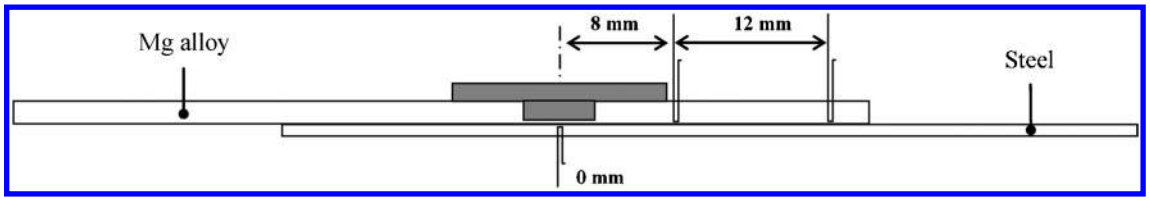

7 Locations of inserted thermocouples for temperature measurement during FSW (3·33 mm s^{-1})

References

1. L. Gaines, R. Cuenca, F. Stodolsky and S. Wu: Proc. of automotive technology development, Detroit, MI, USA, 1996.
2. http://www.twi.co.uk
3. H. K. Mao and P. M. Bell: *J. Geophys. Res.*, 1979, **84**, 4533–4536.
4. L. M. Liu and X. Zhao: *Mater. Charact.*, 2008, **59**, 1279–1284.
5. W. M. Thomas, E. D. Nicholas, J. C. Needham, M. G. Murch, P. Templesmith and C. J. Dawes: GB Patent Application no. 9125978·8, 1991.
6. S. H. C. Park, Y. S. Sato and H. Kokawa: *Scr. Mater.*, 2003, **49**, 161–166.
7. D. Zhang, M. Suzuki and K. Maruyama: *Scr. Mater.*, 2005, **52**, 899–903.
8. A. H. Feng and Z. Y. Ma: *Scr. Mater.*, 2007, **56**, 397–400.
9. C. I. Chang, C. J. Lee and J. C. Huang: *Scr. Mater.*, 2004, **51**, 509–514.
10. W. Woo, H. Choo, D. W. Brown, P. K. Liaw and Z. Feng: *Scr. Mater.*, 2006, **54**, 1859–1864.
11. A. P. Reynolds, W. Tang, T. Gnaupel-Herold and H. Prask: *Scr. Mater.*, 2003, **48**, 1289–1294.
12. C. D. Sorensen, T. W. Nelson and S. M. Packer: Proc. 3rd Int. Symp. on 'Friction stir welding', Kobe, Japan, September 2001, TWI, CD-ROM.
13. L. Cui, H. Fujii, N. Tsuji and K. Nogi: *Scr. Mater.*, 2007, **56**, 637–640.
14. H. Fujii, L. Cui, N. Tsuji, M. Maeda, K. Nakata and K. Nogi: *Mater. Sci. Eng. A*, 2006, **A429**, 50–57.
15. W. M. Thomas, P. L. Threadgill and E. D. Nicholas: *Sci. Technol. Weld. Join.*, 1999, **6**, 365–372.
16. T. J. Lienert Jr, W. L. Stellwag, B. B. Grimmett and R. W. Warke: *Weld. J.*, 2003, **82**, s1–s9.
17. Y. S. Sato, T. W. Nelson, C. J. Sterling, R. J. Steel and C. O. Pettersson: *Mater. Sci. Eng. A*, 2005, **A397**, 376–384.
18. Y. S. Sato, H. Yamanoi, H. Kokawa and T. Furuhara: *Scr. Mater.*, 2007, **57**, 557–560.
19. T. Watanabe, K. Kagiya, A. Yanagisawa and H. Tanabe: *Q. J. Jpn Weld. Soc.*, 2006, **24**, 108–115.
20. H. Kobayashi, K. Nishimoto and K. Ikeuchi: 'Introduction to joining engineering of materials', 182–188; 2002, Tokyo, Sampo.
21. T. B. Massalski: in: 'Binary alloy phase diagrams', 2nd edn, Vol. 3, 2571–2572; 1990, Materials Park, OH, ASM International.